Physics Letters B 291 (1992) 1–6
North-Holland

PHYSICS LETTERS B

Effect of atomic binding on inelastic νe scattering

S.A. Fayans [1], V.Yu. Dobretsov and A.B. Dobrotsvetov
Kurchatov Institute, 123 182 Moscow, Russian Federation

Received 20 March 1992; revised manuscript received 1 July 1992

The energy spectra of electrons knocked out from atoms due to inelastic νe scattering are calculated within the electroweak minimal model, incorporating neutrino electromagnetic form factors. It is shown that these spectra differ significantly from the free scattering ones not only at incoming neutrino energies comparable with electron binding, but also at energies being an order of magnitude larger. For magnetic scattering, the cross sections on bound electrons are always less than on the free ones, and recoil electron spectra at low kinetic energies are naturally cut off. The role of these effects in the scattering of reactor $\bar{\nu}_e$ is demonstrated.

The neutrino–electron scattering is a unique pure weak lepton process which may be studied experimentally in laboratory conditions using various neutrino sources, both terrestrial (β-radioactive nuclei, reactors, accelerators), and extraterrestrial (the Sun, supernova, ...). Hitherto all experimental data on νe-scattering for both muon and electron neutrinos agree with the predictions of the standard minimal electroweak model and, though the accuracy of these data sometimes is not good enough, there is no doubt that this model works excellently. The efforts are now aimed at searching for phenomena beyond the minimal model. Among them are the processes that might be connected with such hypothetic properties of the neutrino as the non-zero neutrino mass and/or anomalously large electromagnetic form factors. This would cause the neutrino oscillations and the helicity flips of neutrinos, thus leading to the space–time evolution of the spin–flavor composition of the neutrino flux. The special interest attached to these phenomena is mainly related to the so-called solar neutrino problem – too low neutrino counting rate in the chlorine-argon experiment [1], about three times less than the standard solar model predictions, and also by a rather strong evidence for anticorrelation of this rate with solar activity [2]. The most attractive explanation for that is the suggestion on the resonant amplification of neutrino oscillations within the Sun [3,4] together with spin and spin–flavor precession [5,6]. This requires that the neutrino would possess at least not too small a magnetic moment. The $\bar{\nu}_e e$-scattering experiments at reactors [7,8] gave the limit [9,10] $\mu_{\bar{\nu}_e} \lesssim 3\times10^{-10}\,\mu_B$, where $\mu_B = e\hbar/2m_e c$ is the Bohr magneton (though see ref. [11], where the use of a more accurate spectrum of reactor $\bar{\nu}_e$ yielded $\mu_{\bar{\nu}_e} = (2\text{–}4)\times10^{-10}\,\mu_B$ for the Reines–Gurr–Sobel experiment [7]). The limit on magnetic moment for electron neutrino, obtained at LAMPF [12], is about a factor of two larger. The analysis of astrophysical data on red giants [13] sets an upper limit to $\mu_{\bar{\nu}}$ of $3\times10^{-12}\,\mu_B$, but even with such a stringent limit the explanation of solar data by the mechanism of spin-flavor precession might be possible [6] though some difficulties still exist [14,15].

Therefore, the direct neutrino magnetic moment measurements or finding even more strict bounds to $\mu_{\bar{\nu}}$ is an extremely urgent task. The only process suitable for these purposes is the νe-scattering, because one can try to detect so small $\mu_{\bar{\nu}}$ values if the contribution of magnetic scattering to the total cross section makes a measurable share of the electroweak cross section, which goes up with the neutrino energy increase; the magnetic scattering cross section diverges logarithmically at a lower detection threshold, which is seen from the example of free νe-scattering [11]. This is why the only way to succeed is to detect recoil electrons with small kinetic energies. Though such experiments are very hard to perform due to

[1] E-mail address: fayans@jbivn.kiae.su.

smallness of effects and poor background conditions, the progress in experimental technique may be so considerable (see, for example, ref. [16]), that such measurements will become possible. Then it will be necessary to adequately take into account the effects of electron binding in atoms.

Here we consider the inelastic low-energy ve scattering on bound electrons accompanied by ionization of the atom. For this process one has the following matrix elements:

$$M_{\mathrm{fi}}^{(\mathrm{w})} = -\frac{G_{\mathrm{F}}}{\sqrt{2}\,\hbar c}\,\bar{u}_{\boldsymbol{p}\lambda_{\nu_2}}\gamma^{\mu}(1+\lambda^5)u_{\boldsymbol{p}\lambda_{\nu_1}} \times \int \mathrm{d}^3r\,\bar{\psi}^{(-)}_{\boldsymbol{p}\lambda_{\mathrm{e}_2}}(\boldsymbol{r})\gamma_{\mu}(g_{\mathrm{V}}+g_{\mathrm{A}}\gamma^5)\psi_{njlm_{\mathrm{e}_1}}(\boldsymbol{r}) \times \exp(-i\boldsymbol{q}\cdot\boldsymbol{r}/\hbar)\,, \tag{1}$$

$$M_{\mathrm{fi}}^{(\lambda)} = -\frac{4\pi e^2\hbar}{c}\,\bar{u}_{\boldsymbol{p}\lambda_{\nu_2}}\frac{\Gamma^{\mu}(q)}{(q^{(0)})^2-(\boldsymbol{q})^2}\,u_{\boldsymbol{p}\lambda_{\nu_1}} \times \int \mathrm{d}^3r\,\bar{\psi}^{(-)}_{\boldsymbol{p}\gamma_{\mathrm{e}_2}}(\boldsymbol{r})\gamma_{\mu}\psi_{njlm_{\mathrm{e}_1}}(\boldsymbol{r}) \times \exp(-i\boldsymbol{q}\cdot\boldsymbol{r}/\hbar)\,. \tag{2}$$

Here Γ^{μ} is the electromagnetic vertex,

$$\Gamma^{\mu}(q) = F_1(q)\gamma^{\mu} - \frac{F_2(q)}{2m_{\nu}c}\,\sigma^{\mu\nu}q_{\nu}\,, \tag{3}$$

where q is the four-momentum transfer. At small q the electromagnetic neutrino form factors are

$$F_1(q) = \frac{1}{6}\frac{q^2}{\hbar^2}\langle r^2\rangle, \quad F_2(q) = \frac{\mu_{\nu}}{\mu_{\mathrm{B}}}\frac{m_{\nu}}{m_{\mathrm{e}}}\,. \tag{4}$$

In eqs. (1) and (2) $u_{\boldsymbol{p}\lambda}$ is the amplitude of an incoming ultrarelativistic Dirac neutrino with momentum $\boldsymbol{p}$ and helicity λ ($\lambda_{\nu_1}=-1$). In the standard electroweak model, for the electron neutrino one has $g_{\mathrm{V}}=\frac{1}{2}+2\sin^2\theta_{\mathrm{w}}$ and $g_{\mathrm{A}}=\frac{1}{2}$. The contribution of the neutrino charge radius can be carried from eq. (1) to eq. (2) by replacing $g_{\mathrm{V}}\to g'_{\mathrm{V}}=g_{\mathrm{V}}+x$ where $x=\sqrt{2}\,\pi e^2\langle r^2\rangle/3G_{\mathrm{F}}$. The initial electron e_1 is supposed to be in the bound state on the atom subshell with principal quantum number n_1 and angular quantum numbers $j_1 l_1 m_1$. The outgoing electron e_2 is considered to be in the continuum with the momentum $\boldsymbol{p}_2$ at infinity. Its wavefunction, with the spin projection λ_2 on the direction of motion, is represented by the standard expansion using a complete basis of partial waves, the spherical bispinors. In terms of the matrix elements (1) and (2), the differential cross section per one electron can be written as follows:

$$\frac{\mathrm{d}\sigma}{\mathrm{d}T_{\mathrm{e}}}(T_{\mathrm{e}}, E_{\nu_1}, njl_{\mathrm{e}_1}) = \frac{p_{\nu_2}p_{\mathrm{e}_2}}{2^8\pi^5\hbar^5 p_{\nu_1}(2j_1+1)} \times \sum_{m_1}\sum_{\lambda_{\mathrm{e}_2}}\int \mathrm{d}o_{\mathrm{e}_2}\sum_{\lambda_{\nu_2}}\int \mathrm{d}o_{\nu_2}\,|M_{\mathrm{fi}}^{(\mathrm{w})}+M_{\mathrm{fi}}^{(\gamma)}|^2\,, \tag{5}$$

where $T_{\mathrm{e}}=\varepsilon_{\mathrm{e}_2}-m_{\mathrm{e}}c^2$ is the kinetic energy of the recoil electron. Here averaging over the initial electron angular momentum projections and summing over all final states of neutrino and electron are performed.

The wavefunctions and energies of atom bound states were calculated within the relativistic self-consistent Hartree–Fock–Dirac approach with local exchange-correlation potential [17]. The partial radial wavefunctions of outgoing electrons were obtained by a numerical solution of the Dirac equation in the same potential as for the wavefunctions of discrete states.

As target atoms ^{19}F ($Z=9$) and ^{96}Mo ($Z=42$) were chosen. This choice, on the one hand, makes it possible to trace the influence of binding effects from the light atoms to medium ones, and, on the other hand, is explained by the fact that fluorine is contained in scintillation detectors used in experiments being already performed [8], and the atoms with Z close to that of molybdenum may serve in superconductor phase transition calorimeters [16].

In fig. 1 the calculated spectra of recoil electrons knocked out from the K-shell of the ^{19}F atom due to weak and magnetic interactions at an incoming neutrino energy of $E_{\nu_1}=100$ keV are shown. The results of analogous calculations for deep shells of the ^{96}Mo atom are given in fig. 2. For comparison, in the same figures dashed curves are used to present the corresponding cross sections for the free scattering [11,18]:

$$\frac{\mathrm{d}\sigma^{(\mathrm{w})}}{\mathrm{d}T_{\mathrm{e}}} = \frac{G_{\mathrm{F}}^2 m_{\mathrm{e}}}{2\pi\hbar^4c^2} \times [(g'_{\mathrm{V}}+g_{\mathrm{A}})^2+(g'_{\mathrm{V}}-g_{\mathrm{A}})^2(1-T_{\mathrm{e}}/E_{\nu_1})^2 + (g_{\mathrm{A}}^2-g_{\mathrm{V}}'^2)m_{\mathrm{e}}c^2T_{\mathrm{e}}/E_{\nu_1}^2]\,, \tag{6}$$

$$\frac{\mathrm{d}\sigma^{(\mathrm{m})}}{\mathrm{d}T_{\mathrm{e}}} = \frac{\pi e^4\mu_{\nu}^2}{m_{\mathrm{e}}^2c^4}\left(\frac{1}{T_{\mathrm{e}}}-\frac{1}{E_{\nu_1}}\right). \tag{7}$$

As it follows from four-momentum conservation, the

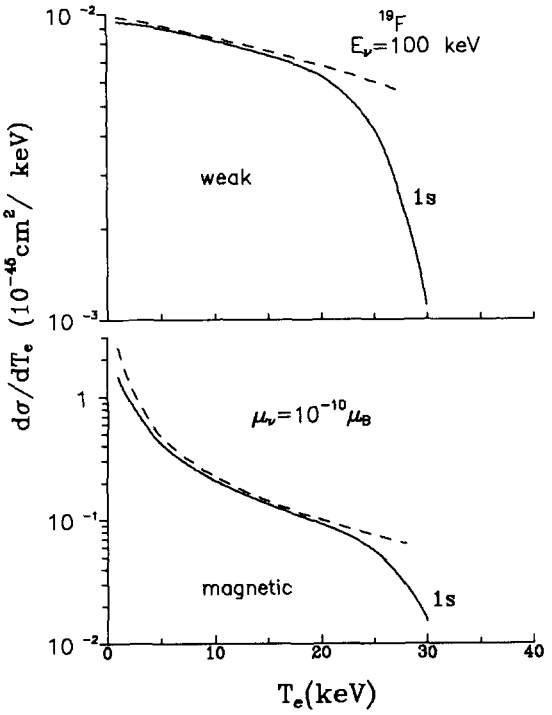

Fig. 1. Spectra of electrons knocked out from the K-shell of a fluorine atom at neutrino energy $E_{\nu_l} = 100$ keV due to weak interaction and neutrino magnetic moment $\mu_\nu = 10^{-10}\mu_B$. The spectra for the free ve scattering are shown by the dashed curves plotted up to the kinematical limit, eq. (8), where they end abruptly.

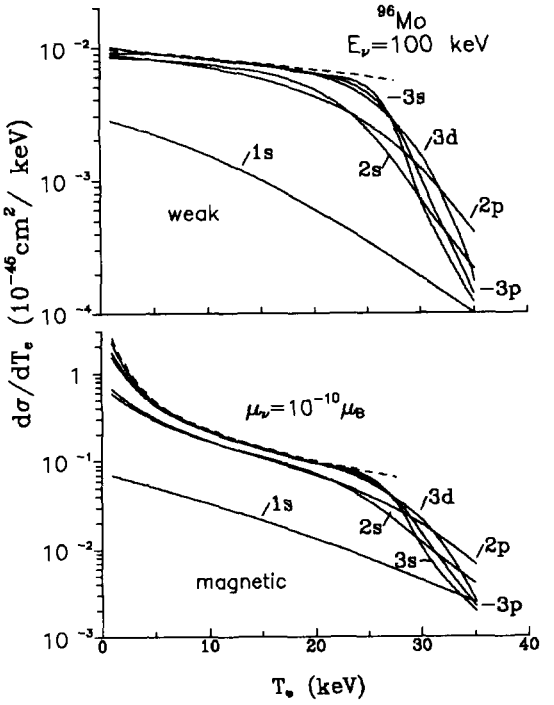

Fig. 2. Spectra of electrons knocked out from the different atomic shells of a molybdenum atom for neutrino scattering at $E_{\nu_l} = 100$ keV. The notations are the same as in fig. 1.

kinetic energy of a recoil electron entering the latter formula is restricted by an upper limit,

$$T_e \leqslant \frac{2E_\nu^2}{2E_\nu + m_e c^2}. \qquad (8)$$

All curves in figs. 1 and 2 and also in the following figures correspond to the cross sections per one electron of a target atom. In all calculations it was supposed that $\mu_\nu = 10^{-10}\,\mu_B$ and $\langle r^2 \rangle = 0$. Calculations were performed with constants taken from ref. [19]. The atomic potential and binding energies of electron subshells were calculated with valence configurations $2p_{1/2}^2 2p_{3/2}^3$ for fluorine and $4d_{3/2}^4 5s_{1/2}^2$ for molybdenum.

As it is seen from fig. 1, at neutrino energy $E_{\nu_l} = 100$ keV the spectra of electrons knocked out from the K-shell of the fluorine atom generally differ insignificantly from the free scattering spectra, which is quite natural, because E_{ν_l} in the given case is more than two orders of magnitude greater than the K-electron binding energy, $\varepsilon_b(1s_{1/2}) = 0.662$ keV. However, even in such a situation the spectra differ noticeably in the region near $T_e \approx 20$ keV, in the vicinity of the upper kinematical limit (8), which is connected with the momentum nonconservation effects in scattering on bound electrons. Such effects causing the smoothing of the hard part of energy spectra of recoil electrons instead of a sharp drop for free scattering, are characteristic for all shells, which can be seen from fig. 2. In this figure, the spectra of recoil electrons knocked out from different shells of a molybdenum atom at the same neutrino energy $E_{\nu_l} = 100$ keV are shown. Noticeable general differences as compared to the free scattering are observed here not only for the deepest 1s-shell with binding energy $\varepsilon_b(1s_{1/2}) = 19.788$ keV, about five times less than the incoming neutrino energy E_{ν_l}, but also for the 2s- and 2p-shells with one order of magnitude lower binding energies [$\varepsilon_b(2s_{1/2}) = 2.798$ keV, $\varepsilon_b(2p_{1/2}) = 2.576$ keV and $\varepsilon_b(2p_{3/2}) = 2.470$ keV]. This can be explained by the fact that the differences between cross sections are

determined by the characteristic momentum nonconservation Δp_e in the scattering process which is of the order of the electron momentum on the considered shell, i.e. $\Delta p_e \approx \alpha Z m_e c/n$, and not by its binding energy $\varepsilon_b \approx -(\alpha Z)^2 m_e c^2/2n^2$. In the energetic scale of T_e this corresponds to the range of $\Delta T_e \approx c^2 p_e \Delta p_e / E_e$ where cross sections $d\sigma/dT_e$ should be distinguished. For the upper end of the recoil spectrum, using eq. (8), one can obtain $\Delta T_e \approx 2(\alpha Z/n) E_\nu (1+y)/(1+2y+2y^2)$, where $y = E_\nu/m_e c^2$. In the nonrelativistic situation one gets $\Delta T_e \approx 2\alpha Z E_\nu/n$. The results shown in figs. 1 and 2 agree well with this estimate. At ultrarelativistic energies one obtains $\Delta T_e \approx \alpha Z m_e c^2/n$. Notice that a relative contribution from the ΔT_e interval decreases in inverse proportion of E_ν. For completeness, we list the binding energies of other subshells relevant to fig. 2: $\varepsilon_b(3s_{1/2}) = 0.479$ keV, $\varepsilon_b(3p_{1/2}) = 0.394$ keV, $\varepsilon_b(3p_{3/2}) = 0.377$ keV, $\varepsilon_b(3d_{3/2}) = 0.277$ keV and $\varepsilon_b(3d_{5/2}) = 0.223$ keV.

The calculated cross sections at all T_e values in figs. 1 and 2 for both weak and magnetic scattering on bound electrons prove to be lower than on the free ones. However, the increase of E_{ν_l} brings the situation with weak scattering to the reverse one, and the corresponding cross section $d\sigma/dT_e$ on atoms start to exceed the free scattering cross section. This is demonstrated in figs. 3 and 4, showing the spectra of recoil electrons knocked out from the K-shells of molybdenum at incoming neutrino energies $E_{\nu_l} = 100$, 250 and 500 keV (fig. 3), and the differential cross sections $d\sigma/dT_e$ for the same electrons at fixed recoil energies $T_e = 10$, 50 and 100 keV in a wider region of E_{ν_l} up to 10 MeV (fig. 4). As it is seen fig. 3, the weak cross section at $E_{\nu_l} = 250$ keV on K-electrons is a little lower than on free ones, and at $E_{\nu_l} = 500$ keV it is a little larger; noticeable differences are observed only near the upper edge of the spectra. The mentioned exceeding of $d\sigma/dT_e$ over free weak scattering, as seen from fig. 4, is also preserved at greater E_{ν_l}, though it is not too large [$\approx (5\text{–}10)\%$].

As for the magnetic scattering, the cross sections for bound electrons prove to be always lower than for the free ones. Here, the most important effect is that, for the scattering on bound electrons, the natural cutoff the divergency of recoil spectrum (7) at low T_e takes place. The reason for that is simple: when a free electron becomes bound and acquires the binding energy ε_b, T_e should be substituted by $T_e + \varepsilon_b$ in (7) at

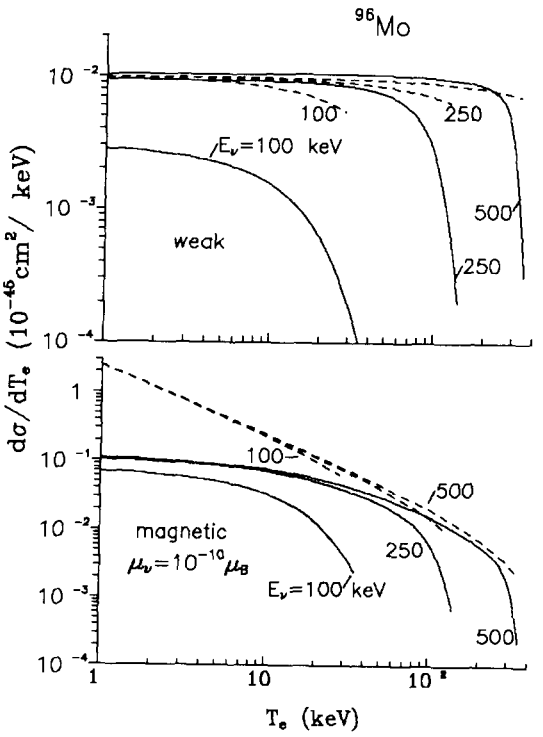

Fig. 3. Spectra of electrons knocked out from the K-shell of a molybdenum atom for neutrino scattering at $E_{\nu_l} = 100$, 250 and 500 keV (shown near the curves). The notations are the same as in fig. 1.

$T_e \to 0$. As a result one should expect that the ratio of two cross sections at $E_{\nu_l} \gg T_e$ will be determined by the factor $(T_e + \varepsilon_b)/T_e$ and the spectrum of electrons in the low energy region at $T_e \to 0$ should reach the plateau. The calculation results shown in figs. 3 and 4 fully agree with these expectations.

Now let us consider what might be the effects of atomic binding in reactor antineutrino $\bar{\nu}_e$ scattering by electrons. A nuclear reactor is considered as a most suitable source for the $\bar{\nu}e$-scattering study. A typical nuclear power plant reactor emits $\approx 5 \times 10^{20}$ $\bar{\nu}_e$ per second with comparatively low energies: the energy spectrum of reactor $\bar{\nu}_e$ spreads up to about 10 MeV and has a maximum at $E_{\bar{\nu}_e} \approx 1$ MeV. The quantity to be measured is the recoil electron spectrum,

$$\frac{\overline{d\sigma}}{dT_e} = \int_{E^{\min}_{\bar{\nu}e}(T_e)}^{\infty} n(E_{\bar{\nu}_e}) \frac{d\sigma(E_{\bar{\nu}_e})}{dT_e} dE_{\bar{\nu}_e}, \qquad (9)$$

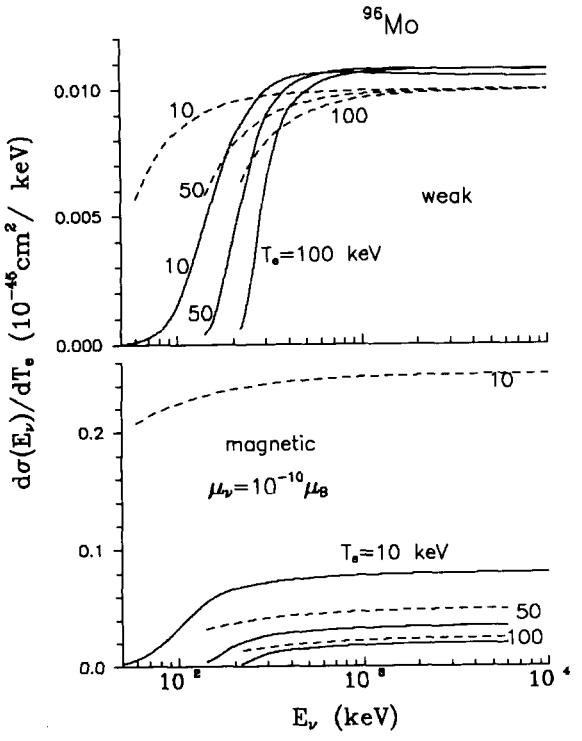

Fig. 4. The differential cross sections for neutrino scattering on the K-electron of a molybdenum atom as a function of incoming neutrino energy E_{ν_l} at fixed recoil kinetic energies $T_e=10$, 50 and 100 keV (shown near the curves). The notations are the same as in fig. 1.

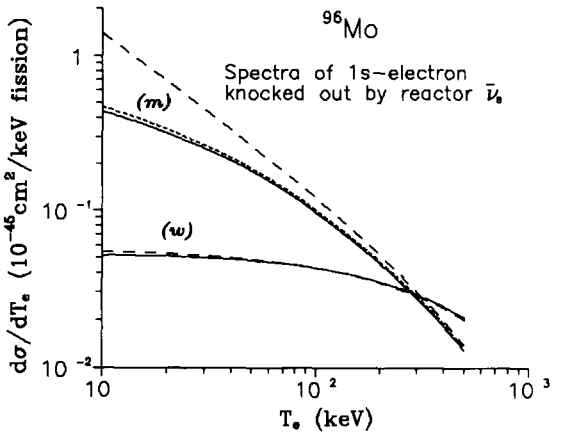

Fig. 5. Spectra of electrons knocked out from the K-shell of a molybdenum atom by reactor $\bar{\nu}_e$ due to weak (w) and magnetic (m) interactions. The calculations are made at $\mu_{\bar{\nu}_e}=10^{-10}\mu_B$ with the $\bar{\nu}_e$ spectrum from ^{235}U fission fragments [11]. The dashed curves are for the free scattering, the solid ones, the exact calculations. The dotted curve is obtained by multiplying the free magnetic scattering cross section by the factor $T_e/(T_e+\varepsilon_b)$, where ε_b is the binding energy of K-electrons in ^{96}Mo.

where $n(E_{\bar{\nu}_e})$ is the reactor $\bar{\nu}_e$ spectrum, and the integration over $E_{\bar{\nu}_e}$ is carried out from the lower limit $E^{\min}_{\bar{\nu}_e}$, determined for free electrons scattering from (8) at fixed kinetic energy T_e, or, for the bound electron scattering, from energy conservation, $E^{\min}_{\bar{\nu}_e}=T_e+\varepsilon_b$. We have calculated the differential cross section (9) for the electrons knocked out from the K-shell of the ^{96}Mo atom using the reactor $\bar{\nu}_e$ spectrum of fission fragments of ^{235}U from ref. [11]. Fig. 5 shows the results for the $10\leqslant T_e\leqslant 500$ keV region. It is seen that for weak scattering the atomic binding effects are insignificant. At the same time for magnetic scattering these effects, as should be expected, reveal themselves quite noticeably, especially at low T_e. To a good approximation they may be simply accounted for by multiplying the free magnetic scattering cross section by the factor $T_e/(T_e+\varepsilon_b)$, as seen from comparison of the dotted curve in fig. 5 with the exactly calculated one: their difference is about 7.5% and 4% at $T_e=10$ keV and $T_e=500$ keV, respectively. These differences can be further reduced by a factor of ≈ 2 if the replacement $T_e\to T_e+\varepsilon_b$ in eq. (7) is used before integration over the reactor $\bar{\nu}_e$ spectrum. As for the whole atom, the net binding effect is not so dramatic as shown in fig. 5 because the main portion of the electrons is on the outer shells with smaller binding energies. Thus, the calculated ratios of differential magnetic cross sections, per one electron of a molybdenum atom, to the free ones, are 0.71, 0.91 and 0.98 at $T_e=1$, 10 and 100 keV, respectively (the corresponding ratios for an uranium atom are 0.58, 0.84 and 0.96). This can be explained by the fact that the main contribution to the cross sections comes from the reactor $\bar{\nu}_e$ with rather large energies, $E_{\bar{\nu}_e}\gtrsim 1$ MeV.

We conclude that the studied effects may be important for future experiments on ve scattering and for the data analysis, especially if low-energy radioactive neutrino sources and targets with atoms of medium and heavy elements are used.

We are grateful to E.Kh. Akhmedov and S.V. Tolokonnikov for valuable discussions and to A.A. Soldatov for supplying us a code for atomic structure

calculations. One of us (S.F.) thanks Professor F. von Feilitzsch for the hospitality and stimulating discussions during the visit to the Technische Universität München in May 1991 when this work has been started.

References

[1] R. Davis Jr., talk XXIst Intern. Conf. on Cosmic-ray physics (Adelaide, Australia, 1990).
[2] K. Lande, talk Neutrino-90, 14th Intern. Conf. on Neutrino physics and astrophysics (CERN, Geneva, June 1990).
[3] L. Wolfenstein, Phys. Rev. D 17 (1978) 2369.
[4] S.P. Mikheev and A.Yu. Smirnov, Yad. Fiz. 42 (1985) 1441 [Sov. J. Nucl. Phys. 42 (1985) 913].
[5] M.B. Voloshin, M.I. Vysotsky and L.B. Okun, Zh. Eksp. Teor. Fiz. 91 (1986) 754 [Sov. Phys. JETP 91 (1986) 446]; E.Kh. Akhmedov, Phys. Lett. B 213 (1988) 64; C.-S. Lim and W.J. Marciano, Phys. Rev. D 37 (1988) 1368.
[6] E.Kh. Akhmedov, Phys. Lett. B 257 (1991) 163.
[7] F. Reines, H.S. Gurr and H.W. Sobel, Phys. Rev. Lett. 37 (1976) 315.
[8] G.S. Vidyakin et al., J. Mosc. Phys. Soc. 1 (1991) 85.
[9] S.V. Tolokonnikov and S.A. Fayans, Izv. Akad. Nauk SSSR, Ser. Fiz. 37 (1973) 2667 [Bull. Acad. Sci. USSR, Ser. Phys. 37 (1973) 181].
[10] A.V. Kyuldjiev, Nucl. Phys. B 243 (1984) 387.
[11] P. Vogel and J. Engel, Phys. Rev. D 39 (1989) 3378.
[12] D.A. Krakauer et al., Phys. Lett. B 252 (1990) 177.
[13] G.G. Raffelt, Phys. Rev. Lett. 64 (1990) 2856.
[14] H. Minakata and H. Nunokava, Phys. Rev. D 43 (1991) R297.
[15] A.B. Balantekin and F. Loreti, Phys. Rev. D 45 (1992) 1059.
[16] F. von Feilitzsch, in: Test of fundamental laws in physics, Proc. IXth Moriond Workshop (1989), eds. O. Fackler and J. Tran Thanh Van (Editions Frontières, Gif-sur-Yvette), p. 435.
[17] V.L. Moruzzi et al., Calculated electronic properties of metals (Pergamon, Oxford, 1978).
[18] G. 't Hooft, Phys. Lett. 37 (1971) 195.
[19] Particle Data Group, J.J. Hernández et al., Review of particle properties, Phys. Lett. B 239 (1990) 1.